Some Metallurgical Issues Concerning Austenite Conditioning in Nb-Ti and Nb-Mo Microalloyed Steels Processed by Near-Net-Shape Casting and Direct Rolling Technologies

BEATRIZ LÓPEZ and JOSE M. RODRIGUEZ-IBABE

As thin slab direct rolling technologies are moving to the production of higher quality steel grades, chemical compositions based on Nb-Ti and Nb-Mo become a good option. However, with the use of multiple microalloying additions, the as-cast austenite conditioning becomes more complex. This paper analyzes some of the microstructural features that should be taken into account during the as-cast austenite conditioning in Nb-Ti and Nb-Mo microalloyed steel grades. In the case of Nb-Ti grades, it has been observed that the process parameters during solidification and post-solidification steps affect the austenite evolution during hot rolling. This is due to the differences in the size and volume fraction of TiN particles that can be formed. Fine TiN precipitates have been shown to be able to delay recrystallization kinetics. Moreover, the solute drag effect of Ti cannot be ignored in the case of hyperstoichiometric Ti/N ratios. It is observed that Nb-Ti grades tend to have lower non-recrystallization temperatures compared to Nb grades, which means that pancaking of the austenite is more difficult for these steels. The opposite is observed for the Nb-Mo grades, although in both cases the behavior is affected by the nominal content of Nb.

DOI: 10.1007/s11661-016-3727-9

I. INTRODUCTION

THIN slab direct rolling (TSDR) has become a well-tested production technology that provides a wide range of steel grades. Nevertheless, customer requirements are pushing the present frontier to attain higher qualities and, in a lot of cases, thicker final gages. This requires that different microalloying elements have to be combined with proper thermomechanical processes.

One of the main functions of Nb is to contribute to a proper austenite conditioning during the thermomechanical processing by deforming the steel below the non-recrystallization temperature (T_{nr}) and promoting a pancaked austenite.[1] This provides a fine final microstructure during cooling down. This is not the only role of Nb, as it also can contribute to the overall strengthening of ferrite through precipitation hardening.[2] These functions of Nb can be complemented with the help of other microalloying elements that act on different aspects. For example, Ti in the form of fine TiN particles prevents austenite grain growth between rolling passes, and as a consequence it contributes to higher degree of austenite grain refinement above the T_{nr} temperature.[3] Concerning Mo, this element mainly affects the microstructural constituents that result from the transformation of austenite and it can also refine NbC precipitates,[4,5] while the main contribution of V is as a precipitation strengthening tool during transformation.[6] These are the conventional functions that these microalloyed elements play in a wide range of high-strength low-alloy (HSLA) and advanced high-strength steels (AHSS).

In addition to the main roles of microalloying elements cited above, Ti and Mo can also affect the recovery and recrystallization kinetics of austenite. These elements can intervene in austenite conditioning through various interactions with Nb, both in solid solution or in an Nb(C,N) strain-induced precipitation state.[7–10]

The effect of microalloying elements on the non-recrystallization temperature may be due to two mechanisms: the solute drag effect and the pinning effect due to strain-induced precipitates, the latter usually exerting the stronger influence.[11–14] The presence of Ti and Mo in Nb-based microalloyed steels might affect both mechanisms and thus modify the T_{nr} value, as has been reported.[1] For example, in the case of Nb-Ti grades, the presence of Ti-rich precipitated carbonitrides can modify the amount of Nb in solution available for further strain-induced precipitation, as quantified by Gong *et al.*[15]

In summary, in multiple microalloying additions, the classical interactions between softening mechanisms and strain-induced precipitation that occur in austenite during thermomechanical processes become more complex. Moreover, in the case of TSDR technologies the

BEATRIZ LÓPEZ and JOSE M. RODRIGUEZ-IBABE, Professors, are with Ceit and Tecnun, University of Navarra, Pº de Manuel Lardizabal 15, 20018 San Sebastian, Basque Country, Spain. Contact e-mail: jmribabe@ceit.es

Manuscript submitted January 15, 2016.
Article published online August 22, 2016

coarse initial as-cast austenite grain size and the amount of microalloying elements in solution affect the softening evolution of the deformed austenite. The refinement and subsequent conditioning of austenite depends on this starting situation.

Although there are different rolling mill configurations based on TSDR technologies, in a high number of industrial plants there are no roughing stands and the thin slab goes directly to the finishing mill. This means that the coarse as-cast austenite grain size must be refined and properly conditioned in only 5-7 passes. In addition, the lower degree of thickness reduction in comparison to conventional Hot Strip Mill (HSM) is another limiting factor. Taking this into account, the chemical composition of the steel and the thermomechanical processing parameters must be selected to fulfill the following aim (Figure 1):

– Complete elimination and refinement of the initial as-cast austenite microstructure in the first rolling stands before the onset of strain-induced precipitation (Refinement stage).
– Once this objective is achieved, the maximum accumulated strain must be obtained in the final part of the rolling mill before transformation (Conditioning stage).

As it becomes more challenging to attain toughness requirements, it is necessary to optimize the austenite conditioning, and this requires a better understanding and quantification of the aforementioned interactions. In the following sections, an analysis of different possible interactions between Nb and Ti or Mo, from the point of view of austenite conditioning, will be discussed. Vanadium has not been considered, as this element has usually a minor effect in austenite evolution during hot working.[4] In the case of Ti, new steel grades based on Ti/N hyperstoichiometric ratios have been developed recently, which implies that this element plays a bigger role in solid solution and also as TiC strain-induced particles during hot working. The analysis will cover hot rolling conditions based on classical Compact Strip Processing (CSP) type configurations with 6-7 stands in the rolling mill.

II. REFINEMENT OF THE INITIAL AS-CAST AUSTENITE

The austenite grain size distributions measured in two thin slabs at the exit of continuous casting are shown in Figure 2. These measurements were taken at the center of thin slabs with a thickness of 60 mm in HSLA quality grades. In the figure, the frequency and the area fraction distributions are drawn based on the equivalent diameter. Although there are some differences between the two thin slabs, the measurements indicate that there is an important fraction of grains coarser than 1 mm. For example, if the area fraction measurements are considered, in both cases more than 40 pct of the total fraction is made up of grains larger than 1 mm. Another characteristic is that the thin slabs show an equiaxed

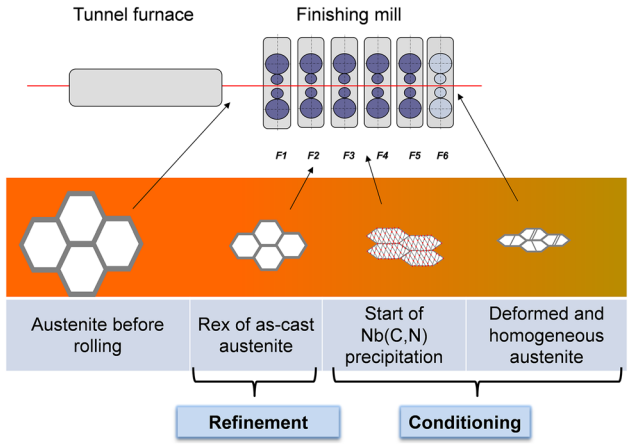

Fig. 1—Illustration of the steps required for austenite conditioning during TSDR thermomechanical processes without roughing passes.

structure at the center, while a more columnar geometry can be observed in regions close to the surface. This coarse austenite microstructure will play a fundamental role in the definition of the process parameters during the initial rolling passes.

The refinement of the as-cast microstructure must be achieved in the initial stages of rolling with the help of both dynamic and static recrystallizations. In the case of plain C-Mn and C-Mn-V steel grades, recrystallization can quickly provide austenite refinement, usually before the entry of the 3rd stand if conventional process parameters are selected.[16] In contrast, in Nb microalloyed grades, both recrystallization mechanisms are more difficult to activate. The combination of coarse initial grain sizes and the solute drag effect of Nb shift the minimum critical strain ε_c for the onset of dynamic recrystallization to high values. In practice, this means that the possibility of refining the coarse grains shown in Figure 2 *via* this mechanism becomes very challenging. In addition, the static recrystallization kinetics is also delayed in comparison to the situation corresponding to plain C-Mn or C-Mn-V grades. Both circumstances have aided the development of specific rules to properly refine the as-cast austenite in Nb grades.[17]

A. *Nb-Ti Steel Grades*

The addition of Ti to Nb-based microalloyed grades introduces several singularities relative to Nb steels that depend on the Ti/N ratio. One of these singularities is the presence of TiN particles with different sizes that can or cannot interact with the austenite microstructure evolution. Some amount of Ti will precipitate as coarse TiN particles (>0.2 μm) mainly during solidification.[18] These particles are ineffective from the point of view of austenite grain growth control and they are detrimental as they can trigger brittle fracture behavior.[19] There are several factors that can minimize their presence, such as low Ti/N ratio and carbon content in the steel.[18] In addition to this, oxide particles[20,21] in the liquid can act as nucleation sites for early TiN formation, as shown in the example of Figure 3. Similarly, the degree of cleanness, which is a function of the amount of sulfur present in the

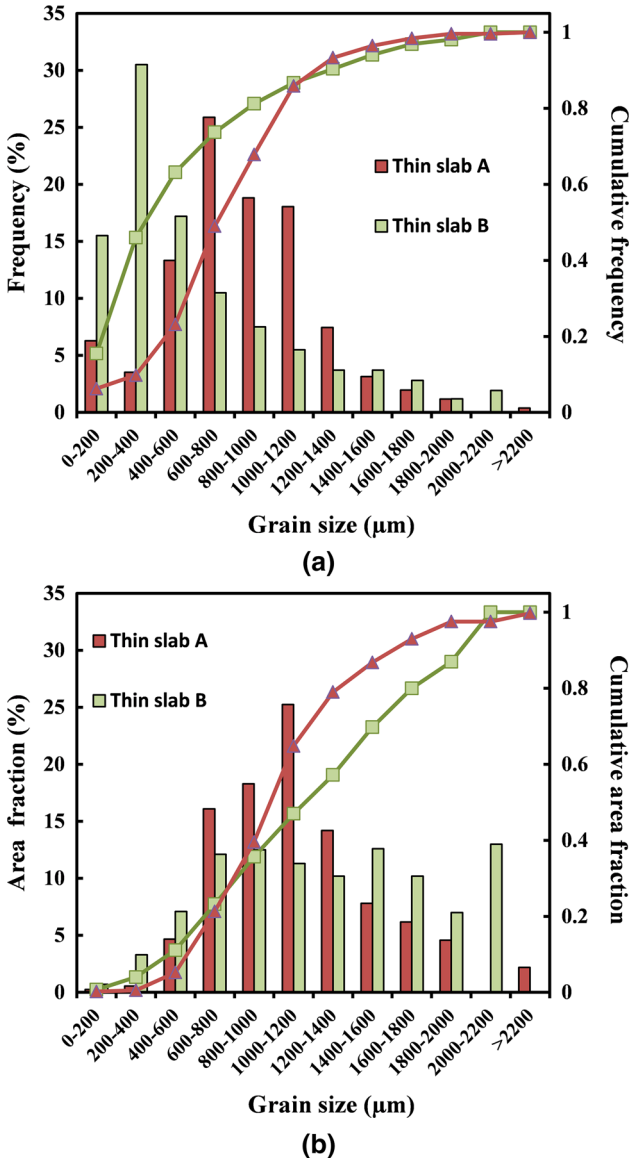

Fig. 2—Austenite grain size distributions at the exit of continuous casting measured in two thin slabs of 60 mm thickness as a function of (*a*) frequency and (*b*) area fraction. The measurements were taken at the center of the thin slab.

steel, can modify the precipitation kinetics of these coarse TiN particles.[22] All these aspects introduce difficulties in the prediction of the volume fraction constituted by coarse particles in relation to the overall TiN precipitation. For example, Figure 4 shows the measurements of coarse TiN particles taken in the center part of two hot-rolled Nb-Ti 12.5-mm-thick coils produced with TSDR technology in different plants. Although there are some differences concerning initial slab thickness and Ti/N ratio, in one of the cases the number of coarse TiN particles present per unit area is about eleven times the particle number found in the other steel. This is a consequence of the process parameters during secondary metallurgy and the start of solidification in the continuous casting.

From the point of view of interaction with the austenite microstructure, the most effective TiN particle precipitation should occur during the post-solidification step in the continuous casting process. In this case, in addition to the Ti/N ratio (steel chemistry), the cooling rate has a significant effect. Recently, the effect of the post-solidification cooling rate was analyzed by Stock *et al.*,[23] extending the initial work of Sage *et al.*[24] to cooling conditions corresponding to near-net-shape technologies. These results are shown in Figure 5, together with other data reported in the literature.[25–27] Without taking other factors into account, if a direct relationship between slab thickness and cooling rate is considered, the mean size of TiN particles could range from 100 nm in a conventional thick slab to ~10 to 20 nm in the case of 50 to 60 mm thin slabs. Similar values have been obtained in other industrial thin slabs, although precise post-solidification rates have not been reported. For example, Nagata *et al.* measured TiN mean particle sizes between 20 and 27 nm for 50 mm thin slabs.[28] Similarly, Bai *et al.* identified that the majority of the particles present in an industrial thin slab were Ti(C,N) precipitates smaller than 20 nm, although some coarse particles (>50 nm) were also detected.[29]

This change in the mean TiN fine particle sizes, close to one order of magnitude, can affect in various ways the microstructural evolution occurring during initial hot working steps when compared to conventional routes. In the aforementioned size interval, the TiN particles control the grain growth of austenite but they can also interact with dynamic and static recrystallization mechanisms. As dynamic recrystallization has a minor effect on the refinement of the coarse as-cast austenite grain sizes in industrial TSDR conditions, attention will be paid to the effect of TiN particles on static recrystallization kinetics.

The interaction between TiN particles and static recrystallization has been analyzed in Ti or Ti-V microalloyed steels and the results reported are contradictory. For example, Leduc and Sellars found that fine TiN particles had little effect on the static recrystallization kinetics and recrystallized grain size compared to plain C-Mn steels.[30] Similarly, Vega *et al.* reported a small effect of Ti on recrystallization.[31] In contrast, Roberts *et al.* found that recrystallization was delayed, particularly after relatively small strains.[32] Finally, Arribas *et al.* described an important delay in the time for 50 pct static recrystallization, $t_{0.5srx}$, which was associated with the presence of fine TiN particles.[26] In all these cases, the analysis was done by simulating conventional reheating procedures in the range of 1473 K to 1523 K (1200 °C to 1250 °C). In these conditions, Ti remains mainly undissolved after reheating.

In addition to fine TiN precipitates, Ti in solution could also affect recrystallization kinetics. Although there has not been a systematic analysis of Nb-Ti steels, different results obtained with hypostoichiometric Ti steels suggest that not all the Ti is precipitated at the entry to the first rolling pass in TSDR configurations. For example, Nagata *et al.* observed that the mean TiN

particle size decreased in some steels after hot rolling process, but increased in others. These differences were associated with the competition between coarsening in some steels and completion of precipitation in others, both of which depend on the Ti and N contents.[28] Similar results have been quantified by Kuhishige *et al.* and Bai *et al.*, suggesting that an important fraction of Ti particles can precipitate during tunnel furnace and initial stages of hot rolling.[29,33] In summary, in hypostoichiometric Ti-based steels there can be an amount of Ti in solution at the entry to the first rolling pass.

Ti in solution during hot rolling introduces an additional delay in recrystallization kinetics through a drag effect. This contribution can be quantified as an additional time increase to that time associated with Nb. In the case of static recrystallization, this dependence can be quantified with the following expressions[34,35]:

$$t_{0.5srx} \propto \exp\left(\left\{\left[\frac{275000}{T}\right] - 185\right\} \cdot [Nb]_{\text{eff}}\right), \quad [1]$$

$$[\text{Nb}]_{\text{eff}} = [\text{Nb}] + 0.374[\text{Ti}] + 0.0585[\text{V}] + 0.027[\text{Al}], \quad [2]$$

where [M] corresponds to the amount (in weight percent) of the specific element in solid solution during hot rolling. As observed, the solute drag due to Ti in solution is small compared to that exerted by Nb.

In the case of hypostoichiometric Ti/N ratios and for a typical amount of N (in the range of 40 to 70 ppm), Eq. [2] predicts that the contribution of Ti to the solute drag effect could be equivalent to an increase of ~0.01 pct in the total effective Nb content. In this context, Uranga *et al.* performed laboratory thermomechanical tests with a hypostoichiometric Ti steel with an initial mean grain size of 700 μm, similar to that corresponding to TSDR conditions, and a TiN particle mean size of 99 nm.[36] The static recrystallization kinetics of austenite was similar to that of a plain C-Mn steel when the deformation was applied in the temperature range corresponding to initial rolling passes, although some amount of Ti was in solution. The presence of Ti in solution was confirmed because in tests done at lower temperatures fresh strain-induced precipitates were identified. In summary, the solute drag effect exerted by Ti is not relevant from the point of view of static recrystallization kinetics.

If solute drag due to Ti has a minor effect on recrystallization kinetics in the case of hypostoichiometric Ti/N ratios, the delay, when present, should be associated with fine TiN particles formed during the post-solidification step. The interaction between precipitates and recrystallization can be analyzed in terms of the driving forces related to both mechanisms.[13] The driving force for recrystallization (F_{rex}) is the stored energy of deformation, expressed as

$$F_{\text{REX}} = \frac{1}{2}\rho\mu b^2, \quad [3]$$

where μ is the temperature-dependent shear modulus of austenite, b is the Burgers vector, and ρ is the dislocation density associated with deformation, which can be estimated as follows[37]:

$$\rho = \left[\frac{\sigma - \sigma_y}{M\alpha\mu b}\right]^2, \quad [4]$$

where σ and σ_y are the flow and yield stress at the deformation temperature, respectively, M is the Taylor factor (3.1 for FCC crystals), and α is a constant taking a value of approximately 0.15. For the calculation of the pinning force (F_{PIN}), the following expression, based on the flexible boundary approach, has been proposed[38]:

$$F_{\text{PIN}} = \frac{3\gamma f_V^{2/3}}{\pi r}, \quad [5]$$

where γ represents the austenite grain boundary energy (0.8 J/m^2), f_{V} the precipitate volume fraction, and r the precipitate radius.

The net driving force for recrystallization is given by the difference between F_{REX} and F_{PIN}. When the pinning force exerted by the precipitates overcomes the stored deformation energy, $F_{\text{PIN}} > F_{\text{REX}}$, recrystallization stops completely, as occurs when strain-induced precipitation is present. In the case of non-fresh precipitates, such as with fine TiN particles that can be present before rolling, the situation can be in the form of $F_{\text{REX}} > F_{\text{PIN}}$, in which grain boundary migration can take place but at some overall reduced velocity relative to free-particle situations.

This qualitative approach can provide some insight regarding the discrepancies observed in the literature. According to Eq. [5], F_{PIN} depends simultaneously on particle size and volume fraction. As indicated in Figure 5, the mean size of fine TiN particles formed during post-solidification depends on the thin slab thickness and corresponding cooling rate. That is, the size can be predicted for a given industrial continuous casting condition. In contrast, the volume fraction of the particles able to interact with recrystallization depends, in addition to Ti and N contents, on the amount of coarse TiN particles previously formed. And, as indicated previously, steelmaking process plays a relevant role.

Figure 6 shows the experimental values for the time to obtain 50 pct static recrystallization for various hypostoichiometric Ti microalloyed steels with different TiN fine particle sizes prior to hot deformation.[26,34,36] For comparison purposes, the behavior corresponding to a plain C-Mn and a 0.05 pct Nb steel are drawn based on the equation obtained by Fernandez *et al.*[34] In the case of 0.05 pct Nb steel, the prediction only includes the solute drag effect associated with this element. The figure shows that a Ti steel with TiN mean particle size of 99 nm behaves like a plain C-Mn grade with no additional delay. Only at the lowest deformation temperature [1323 K (1050 °C)], when some strain-induced precipitation can occur, is recrystallization delayed significantly with respect to the previous tendency. In contrast, the results obtained with mean TiN particles of 12 and 41 nm clearly deviate from the previous

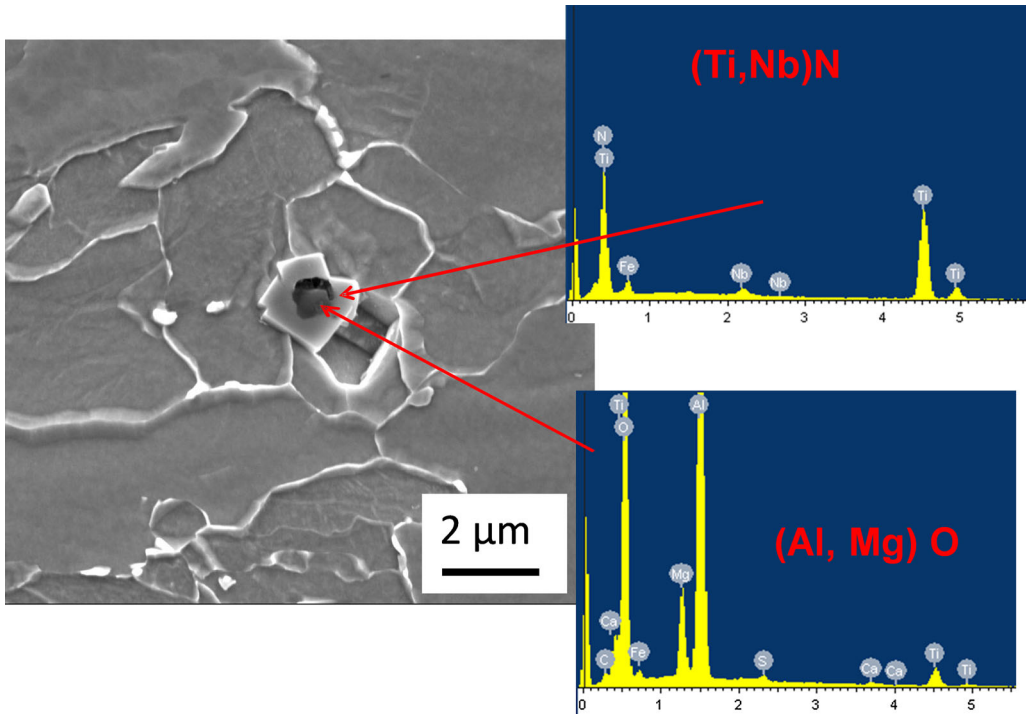

Fig. 3—A (Ti,Nb)N coarse particle nucleated at an oxide in an industrial Nb-Ti microalloyed steel produced through the TSDR process.

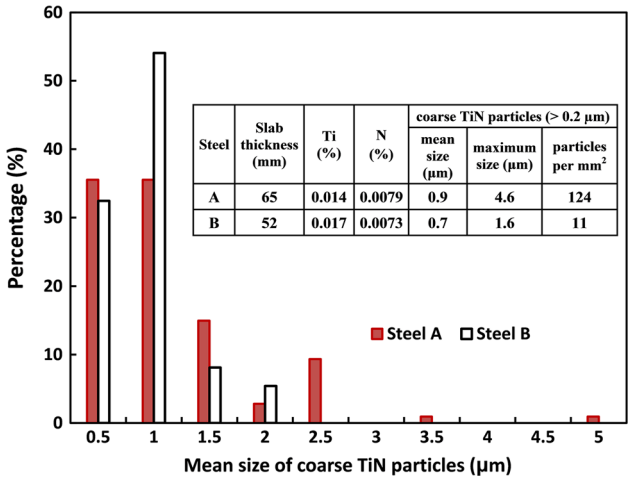

Steel	Slab thickness (mm)	Ti (%)	N (%)	coarse TiN particles (> 0.2 µm)		
				mean size (µm)	maximum size (µm)	particles per mm^2
A	65	0.014	0.0079	0.9	4.6	124
B	52	0.017	0.0073	0.7	1.6	11

Fig. 4—Coarse TiN particle measurements in two industrial samples obtained through the thin slab route.

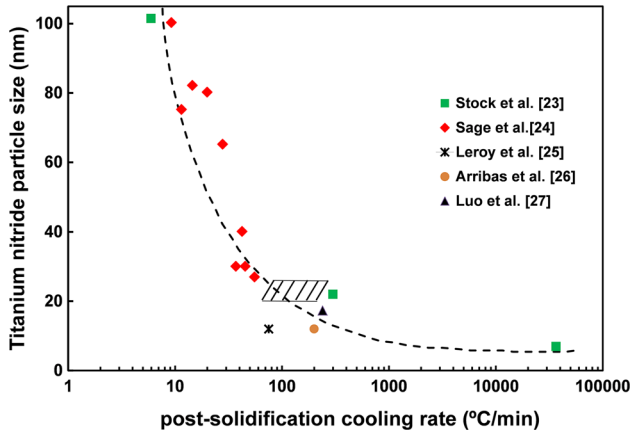

Fig. 5—Relationship between the post-solidification cooling rate and the mean size of fine TiN particles. The dashed interval corresponds to industrial thin slab conditions where cooling rates have not been reported.

tendency. In the range of temperatures usually selected in initial TSDR rolling passes [1323 K to 1353 K (1050 °C to 1080 °C)], the delay due to these particles is in the range associated with 0.05 pct Nb solute drag, while at temperatures lower than 1298 K (1025 °C) the delay associated with the solute drag of Nb is more pronounced. These results confirm that fine TiN particles can introduce a delay that should be added to that caused by the solute drag effect of Nb in solution.

In recent years, there has been a tendency to increase the thickness gage of the final product, which has favored the approach that increases the initial slab thickness from 55 to 60 mm to values in the range of 80 to 100 mm or thicker. As this change affects the post-solidification cooling rate during continuous casting, there will be a tendency for TiN particle sizes to move toward coarser mean values for a given chemical composition. This implies that the thickness of the slab could affect the recrystallization kinetics during initial hot rolling passes. It is possible that, as in conventional rolling, TiN particles can stop grain growth but their role in recrystallization kinetics becomes secondary. This has been confirmed in the results obtained by Sha *et al.* with a Ti/N = 4.3 ratio.[39,40] The static recrystallization kinetics obtained in the case of a medium slab of 170 mm thickness assigned a minor role to the TiN precipitates.

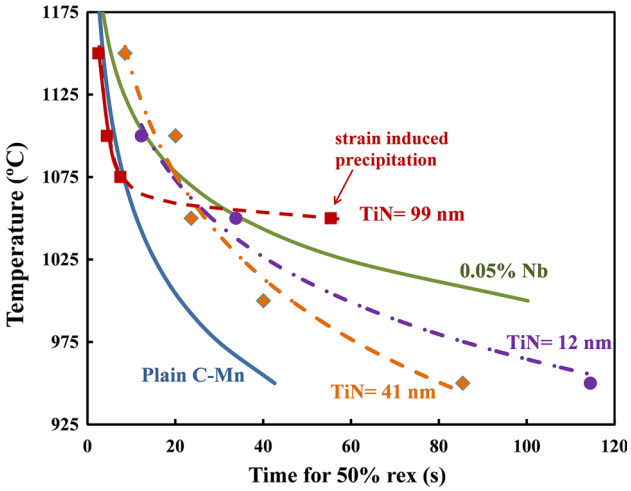

Fig. 6—Effect of different initial microalloying conditions on the time needed for 50 pct static recrystallization (ε = 0.3 and strain rate 1 s^{-1}).[26,34,36] Experimental data corresponding to TiN particle sizes of 12 and 41 nm were corrected for comparison proposes to an initial austenite grain size of D_o = 700 μm. Solid lines represent the behavior associated with conventional C-Mn grades or solute drag effect, while dashed lines correspond to the delay exerted by fine particles.

For Ti contents in the range of hyperstoichiometric Ti/N ratios, the complexity is again related to predicting the amount and size of fine TiN particles and the available Ti in solution during the thermomechanical process. The affinity of Ti with other elements, such as nitrogen and sulfur, requires that its effective amount be quantified as follows:

$$Ti_{eff} = Ti_{total} - 3.4(N) - 3(S). \quad [6]$$

As the Ti/N ratio increases, the mean size of fine TiN particles precipitated during post-solidification step also tends to increase, although there is no direct relationship. For example, for a Ti/N = 6.0 ratio Nagata *et al.* obtained a mean size particle of 27.1 nm in an industrial thin slab quenched at the exit of the tunnel furnace, which is very similar to the values measured in hypostoichiometric steels.[28] In contrast, in an analysis that considered a wide range of Ti/N values, Mao *et al.* reported a change in the TiN mean size from 30 to 60 nm when the Ti amount increased from hypostoichiometric contents to hyperstoichiometric values as high as Ti/N $\cong$ 17.[41] These results suggest that as Ti/N ratio increases, the role of fine TiN particles in static recrystallization kinetics should decrease. In summary, as Ti content increases in hyperstoichiometric Nb-Ti grades, it can be considered that the role of Ti in the refinement of the as-cast grains will be mainly related to its solute drag effect. This could be quantified through expressions like those described in Eqs. [1] and [2].

B. *Nb-Mo Steel Grades*

The presence of Mo in Nb-Mo grades contributes to recrystallization delay through a solute drag effect. From the practical point of view, dynamic recrystallization in Nb-Mo grades plays a minor role in the as-cast austenite grain size refinement, similar to what happens with Nb-Ti grades.[42] That is, static recrystallization is the key factor in achieving a good austenite refinement prior to strain accumulation.

The solute drag of Mo on static recrystallization kinetics is evaluated in Figure 7 by considering the following expressions reported by Isasti *et al.* in combination with Eq. [1][43]:

$$[Nb]_{eff} = [Nb], \text{for Nb microalloyed steels}, \quad [7]$$

$$[Nb]_{eff} = 1.19[Nb] + 0.09[Mo], \text{for0.03 pctNb} - \text{Mo microalloyed steels}, \quad [8]$$

$$[Nb]_{eff} = 1.19[Nb] + 0.032[Mo], \text{for0.06 pctNb} - \text{Mo microalloyed steels}. \quad [9]$$

As observed in the expressions, there is a synergetic effect and the presence of Mo increases the delay due to Nb in solution. In the figure, the multiplying factor on the time for 50 pct static recrystallization due to solute drag effect is drawn as a function of the Mo content for two Nb levels. The temperatures of 1323 K (1050 °C) and 1353 K (1080 °C) were selected as being representatives of those usually present in industrial conditions during initial rolling passes in TSDR configurations. The results clearly indicate that Mo addition can exert a significant delay as temperature decreases.

A delay in the recrystallization kinetics can affect the start of Nb(C,N) strain-induced precipitation. It must be taken into account that the dependence of applied strain ε on recrystallization kinetics ($t_{0.5srx} \sim \varepsilon^{-2}$, if a mean grain size of 800 μm is selected[34]) is greater than its dependence on precipitation kinetics ($t_{0.05p} \sim \varepsilon^{-1}$, where $t_{0.05p}$ represents the time required for 5 pct precipitation[44,45]). But in a non-isothermal condition, as occurs between rolling passes, the decrease in temperature could favor premature precipitation before the refinement of the as-cast grains is completed. Taking this into account, new thin slab direct rolling concepts have been proposed to assure a complete austenite refinement prior to Nb(C,N) precipitation.[46]

III. AUSTENITE CONDITIONING (PANCAKING)

Once the initial as-cast austenite has been refined, the aim of the second stage of austenite conditioning is to accumulate as much strain as possible in the austenite to end up with a pancaked structure, which is favorable for obtaining a refined final ferrite microstructure after cooling. As in the previous section, a distinction between Nb-Ti and Nb-Mo grades will be considered.

The non-recrystallization temperature, T_{nr}, is a parameter that helps analyze the recrystallization-precipitation interactions during thermomechanical processes. In general, the objective is to obtain high T_{nr} temperatures in order to have sufficient rolling passes to

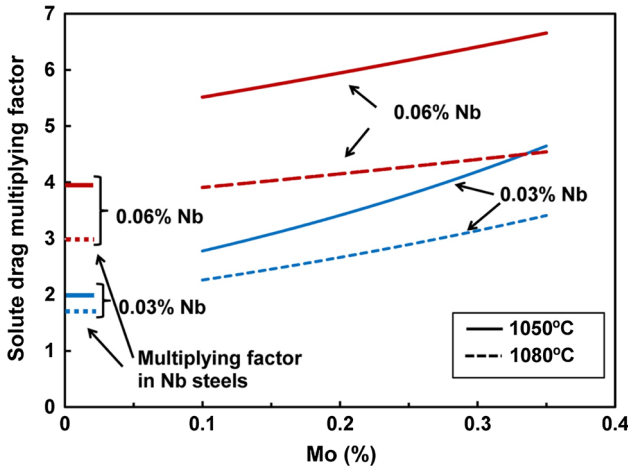

Fig. 7—Multiplying factor on the time for 50 pct static recrystallization due to solute drag effect as a function of the Mo amount in Nb-Mo steel grades.

accumulate the required strain in austenite before transformation. As the T_{nr} temperature depends on the recovery-recrystallization-precipitation interactions, the steel chemical composition and the hot rolling process parameters have a determining role.

A. *Nb-Ti Steel Grades*

Figure 8 summarizes the T_{nr} temperature values obtained with different Nb, Ti, and Nb-Ti heats by performing multipass torsion tests as a function of the strain per pass. The analysis considers different soaking conditions and interpass times.[26,47,48] In Figures 8(a) and (b), the results confirm that Ti as the sole microalloying element is less effective in achieving high T_{nr} values than Nb or Nb-Ti combinations. For the case of initial soaking temperatures of 1473 K to 1535 K (1200 °C to 1250 °C) (Figure 8(a)), although different Ti/N ratios are considered, all the data concerning Nb-Ti heats do not show specific tendencies and remain inside a temperature interval that decreases as the applied strain per pass increases.

When higher soaking temperatures are considered [1673 K to 1733 K (1400 °C to 1460 °C)], a slight increase in T_{nr} is observed in the Ti steels (when compared to the results illustrated in Figure 8(a)), but they remain lower than those obtained in the Nb grades. This increase in the non-recrystallization temperature was assigned to an additional solute drag effect exerted by the higher amount of Ti put into solution during soaking.[47]

Figure 8(c) compares the situation corresponding to Nb and Nb-Ti heats with similar Nb contents. When Ti is added to a Nb steel, the T_{nr} temperature remains constant or decreases. This decrease is more pronounced as Nb content increases. This is due to both a reduction of the Nb content in solution (part of Nb precipitated before rolling as (Nb,Ti)(C,N) particles)[49] and Nb(C,N) heterogeneous nucleation onto TiN coarse particles.[50] One example of this is shown in Figure 9.

In the case of hyperstoichiometric Ti/N ratios, it might be considered that TiC strain-induced precipitation may affect T_{nr} temperature. In the results shown in Figure 8, it is not possible to draw conclusions when comparing hypo- or hyperstoichiometric Ti/N ratios, as the T_{nr} value seems to be more dependent on the Nb content. It has been reported that TiC strain-induced precipitation can take place at temperatures lower than 1223 K (950 °C) after quite long times,[41] which suggests some practical difficulties in properly accumulating strain during the last rolling passes in TSDR configurations. Modeling predictions made by Wang *et al.* confirm that for the case of low C grades, TiC strain-induced precipitation can mainly occur with low temperature finishing rolling strategies.[51] Jung *et al.* analyzed the carbide precipitation behavior during austenite deformation in a Ti-Nb-V microalloyed steel with Ti/N~5.9.[52] Using PTT (precipitation-time-temperature) diagrams, they observed that the nose of the curve was in the range of 1233 K (950 °C) within quite short time periods and that the precipitates were Nb-rich (Nb,Ti)C carbides. All these observations agree with the behavior observed in Figure 8(b) for the evolution of the non-recrystallization temperature.

B. *Nb-Mo Steel Grades*

Figure 10 shows that the addition of Mo to Nb microalloyed steels can modify the non-recrystallization temperature.[53] These results have been obtained following an experimental procedure similar to the one used for the Nb-Ti grades for the condition corresponding to high soaking temperatures [1673 to 1733 K (1400 to 1460°C)] in order to obtain large initial austenite grain sizes and high supersaturation levels of microalloying elements. For purposes of comparison, Figure 10 includes the lines describing the behavior of the Ti steels from Figure 8(b).

For the 0.03 pct Nb content, the addition of Mo results in an increase of ~30 K (30 °C) in the T_{nr} temperature, which remains constant in the analyzed pass strain interval. In contrast, when the Nb content was increased to 0.06 pct, the addition of Mo (0.16 or 0.31 pct) did not show any change in the non-recrystallization temperature. It is important to observe that in the steels with both Nb contents, there are no differences between the addition of 0.16 or 0.31 pct Mo.

This influence of Mo on the T_{nr} temperature has been related to the retardation of recrystallization kinetics due to the solute drag effect.[53] By comparing austenite evolution modeling predictions with experimental results, it has been concluded that the solute drag effect can determine the non-recrystallization temperature in the Nb-Mo steels in some specific conditions that depend on the applied strain and interpass time.[53] For example, in the range of medium Nb contents (0.03 pct Nb), it was observed that the additional solute drag effect exerted by Mo allowed the T_{nr} values to be higher in the Nb-Mo than in the Nb steels. In this situation, Nb(C,N) strain-induced precipitation occurs at lower temperatures than T_{nr} in Nb-Mo grades. The difference between both temperatures can be in the

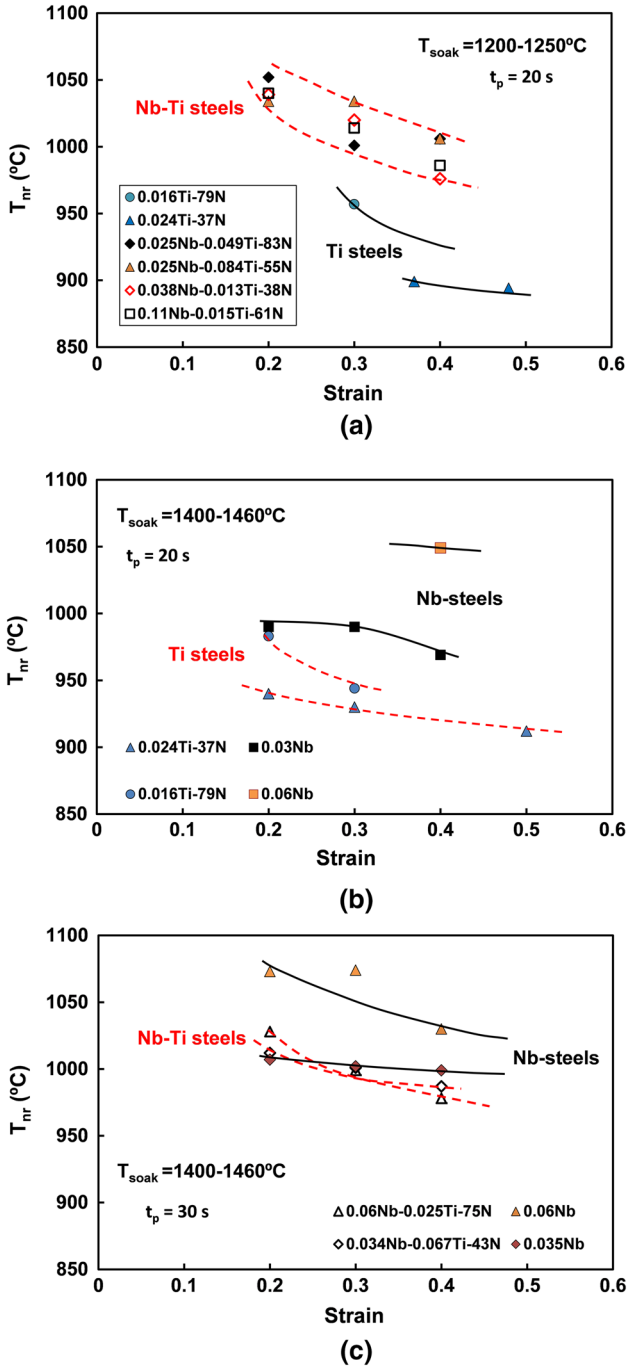

Fig. 8—Non-recrystallization temperatures of several Nb, Ti, and Nb-Ti steels as a function of deformation parameters. (*a*) Initial soaking temperatures of 1473 K to 1535 K (1200 °C to 1250 °C), (*b*) initial soaking temperatures of 1673 to 1733 K (1400 °C to 1460 °C), and (*c*) comparison between Nb and Nb-Ti steels with similar Nb contents.

range of 40 K to 70 K (40 °C to 70 °C) and it depends on the applied strain per pass. However, when the Nb content increases to 0.06 pct Nb, the acceleration of Nb(C,N) strain-induced precipitation makes the contribution of Mo, as solute drag, less relevant. In this case, the T_{nr} temperature is defined by the onset of strain-induced precipitation.

With regard to the nature of strain-induced particles, in thermomechanical laboratory simulations done with Nb-Mo grades, Pereda identified the particles as Nb(C,N) precipitates in samples quenched immediately from the temperature interval between T_{nr} [1299 K (1026 °C)] and 1173 K (900 °C).[54] In contrast, in relaxation tests done at 1123 K (850 °C), Yuan *et al.* observed that Mo was present in Nb(C,N) precipitates.[55] In this context, recent analyses by Enloe *et al.* indicate that very little Mo usually incorporates into Nb-rich carbonitrides in austenite.[56] On the other hand, it has been reported that Mo can delay the Nb(C,N) precipitation kinetics by reducing the activity of C and N.[7] Nevertheless, both aspects require further quantitative analysis.

IV. DISCUSSION

Steel chemistries based on Nb-Ti and Nb-Mo become a good option for TSDR technologies when high mechanical properties are required. The contribution of the mechanisms that determine the total strength of the hot-rolled product can be different depending whether Ti or Mo is selected, but in addition to this, their role during the austenite refinement and pancaking steps can vary markedly.

The results described previously indicate that Ti or Mo additions to Nb grades delay the refinement of the austenite as-cast microstructure. This delay can be due to the presence of fine particles (TiN precipitates) and to solute drag (Ti and Mo in solution).

In relation to the role of fine TiN particles, the process parameters during solidification and post-solidification steps need to be considered in addition to the chemistry (Ti and N contents). Figure 5 suggests that it is possible, for a given slab thickness, to evaluate whether the size of fine TiN particles can interact with static recrystallization kinetics. In addition to this, as Eq. [5] indicates, it is necessary to know their volume fraction and this remains a more difficult issue. As secondary metallurgy and solidification procedures affect the amount of Ti available to precipitate as fine TiN particles, the behavior can vary from plant to plant and, if there is no well-stabilized procedure in the steelmaking process, from heat to heat. This introduces uncertainty in determining the effect of fine TiN particles on the kinetics of static recrystallization of the as-cast initial austenite grains and its proper quantification and prediction remain today an open question.

Figures 6 and 7 reflect the relevance of the initial rolling temperature to the static recrystallization delays due to solute drag and previously precipitated fine particles. As a consequence, the hot rolling should start at higher temperatures to enhance recrystallization kinetics in Nb-Ti and Nb-Mo steels grades. In addition, time should be also considered as another possibility, mainly because a high number of TSDR industrial plants are not designed to drastically decrease the temperature in the final stands without reducing the entry rolling temperature. This can be implemented by introducing a dummy pass, which differentiates

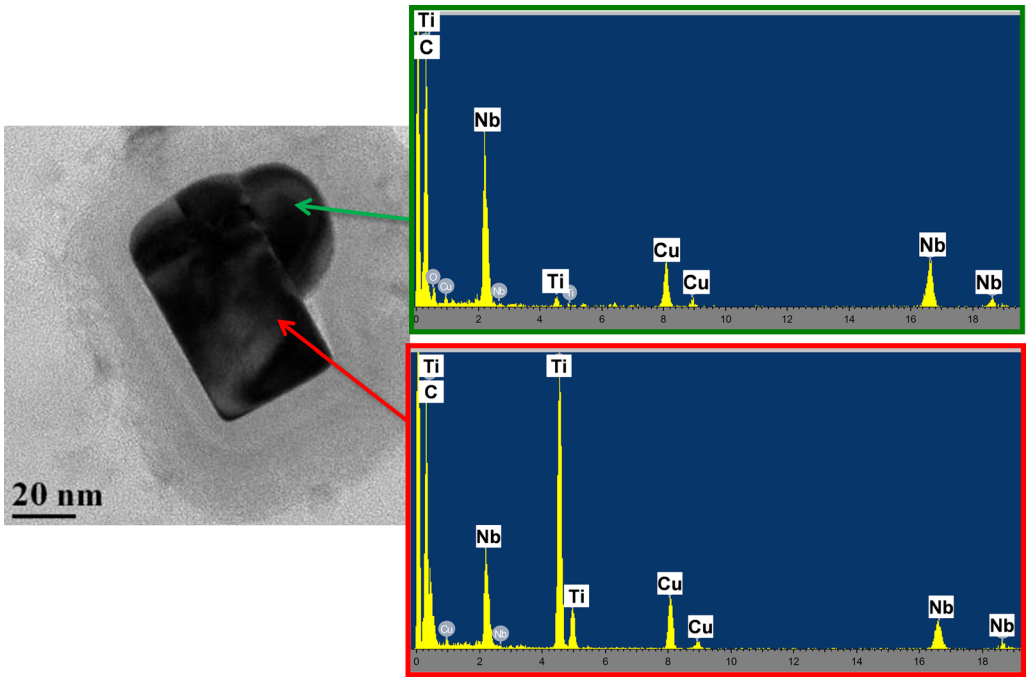

Fig. 9—Nb(C,N) strain-induced precipitate nucleated on a (Ti,Nb)N particle (0.06 pct C, 0.040 pct Nb, 0.010 pct Ti, 73 ppm N).

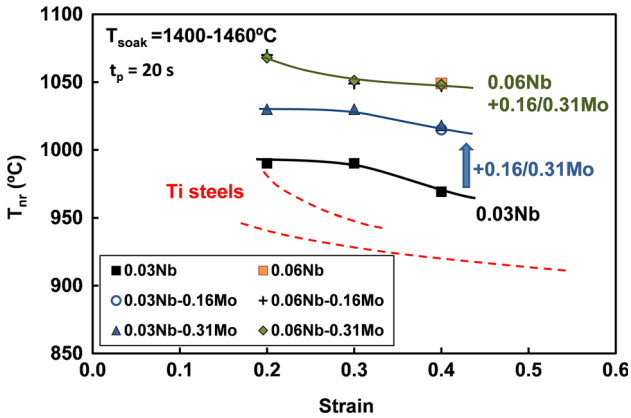

Fig. 10—Dependence of T_{nr} on pass strain (for an interpass time of 20 s) (reprinted with permission from Ref. [53]).

recrystallization passes from the strain accumulation step by a certain amount.

If sufficient austenite refinement is not achieved before the non-recrystallization temperature, a fraction of isolated coarse grains will remain at the exit of the rolling mill. Depending on the microalloying additions and the cooling and coiling strategies, some differences may be present in the final microstructure within Nb-Ti and Nb-Mo steels, which could affect toughness behavior. It has been reported that, due to its tendency to form lower transformation products, Mo can increase the average size of coarse high-angle boundary grains (>15 deg) that provide effective barriers to cleavage fracture. For example, by adding 0.22 pct Mo in an HSLA steel grade and maintaining the rest of the variables constant, Reip *et al.* reported an increase from 21.5 to 30.5 μm in the mean value of the d_{20} parameter in industrial 12.5-mm final gage strips produced by the TSDR technology.[57] The d_{20} parameter represents the grain size for which 20 pct of the area fraction of grains is larger than this value, and it is considered to be a measure of microstructural heterogeneity. This increase in the d_{20} mean value suggests that the coarse austenite grains transform into closely aligned low misorientation bainitic ferrite units that negatively affect toughness in the brittle-ductile regime.[58,59]

In relation to the strain accumulation step in hot rolling, Figure 8 indicates that the pancaking of austenite will be more difficult in Nb-Ti microalloying grades, as there is a tendency for the non-recrystallization temperature to decrease in comparison to Nb grades (Figure 8(c)). The opposite occurs in Nb-Mo grades (Figure 10). In the first case, this appears to be related to Nb coprecipitation on TiN, while in Nb-Mo grades the delay in static recrystallization promoted by Mo in solution can increase the T_{nr} temperature. In both cases, the behavior is affected by the nominal Nb content.

In order to achieve good strength-toughness combinations, for the case of Nb-Mo grades, Isasti *et al.* pointed out the relevance of maximizing the retained strain in austenite during the last rolling passes to increase the fraction of polygonal phases after transformation. This should help reduce the amount of non-polygonal bainitic areas responsible for the increase of microstructural heterogeneity.[60] Similar recommendations have been proposed by Cizek *et al.* for the case of Nb-Mo grades to improve toughness behavior.[61] All these aspects are related to the increase in hardenability associated with Mo addition, and thus Ti-based grades can be less sensitive to this behavior.[62]

Finally, as there is always a fraction of coarse TiN particles (>1 μm) in Nb-Ti steel grades, attention has to be paid to their detrimental effect on toughness. Ray *et al.* determined that, for a given mean TiN particle size, there is a critical grain size below which the cleavage crack propagation is controlled by the ferrite grain size (the effective high-angle misorientation boundary grain size) and above which TiN particle size controls the brittle process.[63] As a consequence, the rolling parameters in the austenite conditioning step should be fixed so as to allow a minimum amount of accumulated strain. And this, again, confirms the relevance of obtaining high T_{nr} temperatures through a proper combination of Nb and Ti amounts and rolling schedules.

V. CONCLUSIONS

The addition of Ti or Mo to Nb microalloyed steels to achieve higher mechanical properties can have important process implications in TSDR routes. The main features to be taken into account are as follows:

- In Nb-Ti steels, Ti can affect the kinetics of static recrystallization in two different ways. For Ti/N<3.4, fine TiN particles can delay the static recrystallization kinetics. Nevertheless, their real effect will depend on the volume fraction of these particles which is affected by secondary metallurgy and solidification conditions. For Ti/N>3.4 grades, the delay in static recrystallization will be due to solute drag, while the TiN particles could have a minor effect. In relation to Nb-Mo steels, Mo will exert an additional delay by solute drag effect.
- The delay in static recrystallization will affect the refinement of the as-cast austenite microstructure at the initial rolling passes. The selection of higher initial rolling temperatures or an increase in the interstand time by the inclusion of dummy passes can be industrial procedures to compensate this effect.
- It is observed that Nb-Ti grades tend to have lower T_{nr} temperatures compared to Nb grades, which means that pancaking of the austenite is more difficult for these steels. The opposite is observed for the Nb-Mo grades, although in both cases the behavior is affected by the nominal content of Nb.
- The effect of coarse remaining austenite grains prior to transformation can be different depending on Ti or Mo selection. In the first case, coarse TiN particles can be the controlling step of the brittle process when they are in the presence of coarse grains, while in Mo-based grades, this element can produce an increase of the average size of coarse high-angle boundary grains (>15 deg) that provide effective barriers to cleavage fracture.

ACKNOWLEDGMENT

Partial financial support of this work by the Basque Government (Elkartek KK-2015/00049 project) is gratefully acknowledged.

REFERENCES

1. S. Vervynckt, K. Verbeken, B. Lopez, and J.J. Jonas: *Int. Mater. Rev.*, 2012, vol. 57, pp. 187–207.
2. M.A. Altuna, A. Iza-Mendia, and I. Gutierrez: *Metall. Mater. Trans. A*, 2012, vol. 43A, pp. 4571–86.
3. D.N. Crowther and W.B. Morrison: *Titanium Technology in Microalloyed Steels*, Institute of Materials, London, 1997, pp. 44–64.
4. M. Militzer, E.B. Hawbolt, and T.R. Meadowcroft: *Metall. Mater. Trans. A*, 2000, vol. 31A, pp. 1247–59.
5. N. Isasti, D. Jorge-Badiola, M.L. Taheri, and P. Uranga: *Metall. Mater. Trans. A*, 2014, vol. 45A, pp. 4960–71.
6. R. Lagneborg, T. Siwecki, S. Zajac, and B. Hutchinson: *Scand. J. Metall.*, 1999, vol. 28, pp. 186–241.
7. B. Bacroix, M. G. Akben and J.J. Jonas: *Proc. of Microalloyed Austenite*, P.J. Wray and A.J. DeArdo, eds., AIME, Warrendale, PA, 1982, pp. 293–318.
8. W.B. Lee, S.G. Hong, C.G. Park, K.H. Kim, and S.H. Park: *Scripta Mater.*, 2000, vol. 43, pp. 319–24.
9. M.G. Akben, B. Bacroix, and J.J. Jonas: *Acta Metall.*, 1983, vol. 31, pp. 161–74.
10. B. Pereda, A. Fernandez, B. López, and J.M. Rodriguez-Ibabe: *ISIJ Int.*, 2007, vol. 47, pp. 860–68.
11. M.G. Akben, I. Weiss, and J.J. Jonas: *Acta Metall.*, 1981, vol. 29, pp. 111–21.
12. J.G. Speer and S.S. Hansen: *Metall. Trans. A*, 1989, vol. 20A, pp. 25–38.
13. O. Kwon and A.J. DeArdo: *Acta Metall. Mater.*, 1991, vol. 39, pp. 529–38.
14. M.D. Kashif: Rehman and H*S. Zurob. Metall. Mater. Trans. A*, 2013, vol. 44A, pp. 1862–71.
15. P. Gong, E.J. Palmiere, and W.M. Rainforth: *Acta Mater.*, 2015, vol. 97, pp. 392–403.
16. JM Rodriguez-Ibabe, P Uranga, and B López: *J. Iron Steel Res. Int.*, 2011, vol. 18 (sup. 1), pp. 459–65.
17. P. Uranga, A.I. Fernandez, B. Lopez, and J.M. Rodriguez-Ibabe: *Mater. Sci. Forum*, 2005, vols. 500–501, pp. 245–52.
18. F.B. Pickering: *Titanium Technology in Microalloyed Steels*, Institute of Materials, London, 1997, pp. 10–43.
19. M.A. Linaza, J.M. Rodriguez-Ibabe, and J.J. Urcola: *Fatigue Fract. Eng. Mater. Struct.*, 1997, vol. 20, pp. 619–32.
20. D.P. Fairchild, D.G. Howden, and W.A.T. Clark: *Metall. Mater. Trans. A*, 2000, vol. 31A, pp. 653–67.
21. V. Descotes, S. Migot, F. Robaut, J.-P. Bellot, V. Perrin-Guérin, S. Witzke, and A. Jardyet: *Metall. Mater. Trans. A*, 2015, vol. 46A, pp. 2793–95.
22. P. Rocabois, J. Lehmann, H. Gaye, and M. Wintz: *J. Cryst. Growth*, 1999, vol. 198 (199), pp. 838–43.
23. J. Stock, C.M. Enloe, RJ O'Malley, K.O. Findley, and JG Speer: *Iron Steel Technol.*, 2014, vol. 11 (June), pp. 180–86.
24. A. M. Sage, R. C. Cochrane, D. Howse: *Proc. Intern. Conf. on Processing, Microstructure and Properties of Microalloyed and other Modern HSLA Steels*, Pittsburgh, PA, USA, 1992, pp. 443–60.
25. V. Leroy and J.C. Herman: *Microalloying 95 Conference Proceedings*, 1995, pp. 213–23.
26. M. Arribas, B. López, and J.M. Rodriguez-Ibabe: *Mater. Sci. Eng., A*, 2008, vol. 485, pp. 383–94.
27. H. Luo, L.P. Karjalainen, D.A. Porter, H.-M. Liimatainen, and Y. Zhang: *ISIJ Int.*, 2002, vol. 42, pp. 273–82.
28. M.T. Nagata, J.G. Speer, and D.K. Matlock: *Metall. Mater. Trans. A*, 2002, vol. 33A, pp. 3099–3110.
29. M. Bai, D. Liu, Y. Lou, X. Mao, L. Li, and X. Huo: *J. Univ. Science Technol. Beijing*, 2006, vol. 13, pp. 230–34.
30. L. A. Leduc and C. M. Sellars: *Proc. Int. Conference on Thermomechanical Processing of Microalloyed Austenite*, Pittsburgh, PA, USA, 1982, pp. 641–54.
31. M.I. Vega, S.F. Medina, A. Quispe, M. Gómez, and P.P. Gómez: *Mater. Sci. Eng., A*, 2006, vol. 423, pp. 253–61.
32. W. Roberts, A. Sandberg, T. Siwecki, and T. Werlefors: *HSLA Steels. Technology and Applications*, ASM, Ohio, 1984, pp. 67–84.
33. K. Kunishige and N. Nagao: *ISIJ Int.*, 1989, vol. 29, pp. 940–46.
34. A.I. Fernández, P. Uranga, B. López, and J.M. Rodriguez-Ibabe: *ISIJ Int.*, 2000, vol. 40, pp. 893–901.

35. Z. Aretxabaleta, B. Pereda, and B. López: *Mater. Sci. Eng., A*, 2014, vol. 600, pp. 37–46.
36. P. Uranga, A.I. Fernández, B. López, and J.M. Rodriguez-Ibabe: *Thermomechanical Processing of Steels*, Institute of Materials, London, 2000, vol. 1, pp. 204–13.
37. B. Dutta, E. Valdes, and C.M. Sellars: *Acta Mater*., 1992, vol. 40, pp. 653–62.
38. E.J. Palmiere, C.I. Garcia, and A.J. DeArdo: *Metall. Trans. A*, 1996, vol. 27A, pp. 951–60.
39. Q.Y. Sha, D.A. Li, and G.Y. Li: *J. Iron Steel Res. Int*., 2014, vol. 21, pp. 232–39.
40. Q.Y. Sha, Z.Q. Sun, and L.F. Li: *Ironmak. Steelmak*., 2015, vol. 42, pp. 74–80.
41. X.P. Mao, Q.L. Chen, and X.J. Sun: *J. Iron Steel Res. Int*., 2014, vol. 21, pp. 30–40.
42. B. Pereda, B. López, and J.M. Rodriguez-Ibabe: *Mater. Sci. Forum*, 2010, vols. 638–642, pp. 687–92.
43. N. Isasti, B. Pereda, B. López, J.M. Rodriguez-Ibabe, and P. Uranga: *Fundamentals and applications of Mo and Nb Alloying in High Performance Steels*, CBMM, IMOA and TMS, London, 2015, vol. 2, pp. 1–28.
44. B. Dutta and C.M. Sellars: *Mater. Sci. Technol*., 1987, vol. 3, pp. 197–206.
45. B. Pereda, J.M. Rodriguez-Ibabe, and B. López: *ISIJ Int*., 2008, vol. 48, pp. 1457–66.
46. C. Klinkenberg, C. Bilgen, J.M. Rodriguez, B Ibabe, B López, and P Uranga: , B. and P.*Mater. Sci. Forum*, 2012, vols. 706–709, pp. 2752–57.
47. R. Abad, B. López and J.M. Rodriguez-Ibabe: *J. Mater. Proc. Technol*., 117/3, CD-ROM Section C4.
48. Ceit, unpublished work.
49. S.G. Hong, K.B. Kang, and C.G. Park: *Scripta Mater*., 2002, vol. 46, pp. 163–68.
50. Y. Lee and B.C. De Cooman: *ISIJ Int*., 2014, vol. 54, pp. 893–99.
51. Z. Wang, Q. Yong, X. Sun, Z. Yang, Z. Li, Ch. Zhang, and Y. Weng: *ISIJ Int*., 2012, vol. 52, pp. 1661–69.
52. J.-G. Jung, J.-S. Park, J. Kim, and Y.-K. Lee: *Mater. Sci. Eng., A*, 2011, vol. 528, pp. 5529–35.
53. B. Pereda, B. López and J.M. Rodriguez-Ibabe: *Proc. Int. Conf. on Microalloyed Steels*, AIST, Warrendale, USA, 2007, pp. 151–59.
54. B. Pereda, Doctoral Thesis, University of Navarra, 2009.
55. S.-Q. Yuan, G.-L. Liang, and X.-J. Guo: *J. Iron Steel Research Int*., 2010, vol. 17, pp. 60–63.
56. C.M. Enloe, K.O. Findley, C.M. Parish, M.K. Miller, B.C. De Cooman, and J.G. Speer: *Scripta Mater*., 2013, vol. 68, pp. 55–58.
57. C-P. Reip, M. Frommert and M. Reifferscheid: *Baosteel BAC Conference*, 2013, J-47.
58. M. Olasolo, P. Uranga, J.M. Rodriguez, and J.M. Rodriguez: Ibabe*B. z. Mater. Sci. Eng. A*, 2011, vol. 528, pp. 559–69.
59. N. Isasti, D. Jorge-Badiola, M.L. Taheri, B. López, and P. Uranga: *Metall. Mater. Trans. A*, 2011, vol. 42A, pp. 3729–42.
60. N. Isasti, D. Jorge-Badiola, M.L. Taheri, and P. Uranga: *Metall. Mater. Trans. A*, 2014, vol. 45A, pp. 4972–82.
61. P. Cizek, B.P. Wynne, C.H.J. Davies, and P.D. Hodgson: *Metall. Mater. Trans. A*, 2015, vol. 46A, pp. 407–25.
62. K. Kamibayashi, Y. Tanabe, Y. Takemoto, I. Shimizu, and T. Senuma: *ISIJ Int*., 2012, vol. 52, pp. 151–57.
63. A. Ray, S. Sivaprasad, and D. Chakrabarti: *Int. J. Fract*., 2012, vol. 173, pp. 215–22.